Science of the Total Environment 500–501 (2014) 72–83

Contents lists available at ScienceDirect

Science of the Total Environment

journal homepage: www.elsevier.com/locate/scitotenv

Mapping carbon storage in urban trees with multi-source remote sensing data: Relationships between biomass, land use, and demographics in Boston neighborhoods

Steve M. Raciti [a,b,*], Lucy R. Hutyra [b], Jared D. Newell [b]

[a] Department of Biology, Hofstra University, Gittleson Hall, Hempstead, NY 11549, United States
[b] Department of Earth and Environment, Boston University, 685 Commonwealth Ave., Boston, MA 02215, United States

HIGHLIGHTS

- Used imagery and LiDAR to develop a high resolution urban biomass map for Boston, MA
- Tree carbon storage was 355 Gg (28.8 Mg C ha^{-1}) for the City of Boston, MA
- No significant correlations between tree biomass and Boston neighborhood demographics
- Dense urban areas can contain considerable tree canopy cover and biomass stocks

ARTICLE INFO

Article history:
Received 30 March 2014
Received in revised form 1 August 2014
Accepted 8 August 2014
Available online xxxx

Editor: Simon Pollard

Keywords:
Urban tree canopy
Vegetation biomass
Carbon cycle
Demographics
High resolution remote sensing
LiDAR

ABSTRACT

High resolution maps of urban vegetation and biomass are powerful tools for policy-makers and community groups seeking to reduce rates of urban runoff, moderate urban heat island effects, and mitigate the effects of greenhouse gas emissions. We developed a very high resolution map of urban tree biomass, assessed the scale sensitivities in biomass estimation, compared our results with lower resolution estimates, and explored the demographic relationships in biomass distribution across the City of Boston. We integrated remote sensing data (including LiDAR-based tree height estimates) and field-based observations to map canopy cover and aboveground tree carbon storage at ~1 m spatial scale. Mean tree canopy cover was estimated to be 25.5 ± 1.5% and carbon storage was 355 Gg (28.8 Mg C ha^{-1}) for the City of Boston. Tree biomass was highest in forest patches (110.7 Mg C ha^{-1}), but residential (32.8 Mg C ha^{-1}) and developed open (23.5 Mg C ha^{-1}) land uses also contained relatively high carbon stocks. In contrast with previous studies, we did not find significant correlations between tree biomass and the demographic characteristics of Boston neighborhoods, including income, education, race, or population density. The proportion of households that rent was negatively correlated with urban tree biomass ($R^2 = 0.26$, $p = 0.04$) and correlated with Priority Planting Index values ($R^2 = 0.55$, $p = 0.001$), potentially reflecting differences in land management among rented and owner-occupied residential properties. We compared our very high resolution biomass map to lower resolution biomass products from other sources and found that those products consistently underestimated biomass within urban areas. This underestimation became more severe as spatial resolution decreased. This research demonstrates that 1) urban areas contain considerable tree carbon stocks; 2) canopy cover and biomass may not be related to the demographic characteristics of Boston neighborhoods; and 3) that recent advances in high resolution remote sensing have the potential to improve the characterization and management of urban vegetation.

© 2014 Elsevier B.V. All rights reserved.

1. Introduction

Urbanization is a significant driver of global environmental change (Imhoff et al., 2004; Foley et al., 2005). In coming decades, increases in global population and socioeconomic advancement in developing nations will accelerate urban expansion. Up to 70% of the global population will live in cities by 2050 (UNFPA, 2007) with urban land cover expanding up to 3 times its current area (Angel et al., 2005; Seto et al., 2011). Urban growth creates widespread ecosystem modification, dramatically altering land cover in and around urbanizing regions. Current estimates of urban area range from 0.2 to 3% of global land cover (Schneider et al., 2010); however, urban ecological footprints and high demand for natural resources lead to modification of ecosystems and land covers at a much broader scale (Seto et al., 2012; Defries et al.,

* Corresponding author at: Department of Biology, Hofstra University, Gittleson Hall, Hempstead, NY 11549, United States. Tel.: +1 516 463 6001; fax: +1 516 463 5112.
E-mail address: Steve.M.Raciti@Hofstra.edu (S.M. Raciti).

http://dx.doi.org/10.1016/j.scitotenv.2014.08.070
0048-9697/© 2014 Elsevier B.V. All rights reserved.

2010; Potere and Schneider, 2007; Alberti et al., 2003; Sadik, 1999). Land cover changes associated with urbanization decrease carbon storage (Seto et al., 2012; Hutyra et al., 2011a; Imhoff et al., 2004), alter biogeochemical cycles (Grimm et al., 2008; Pataki et al., 2006; Kaye et al., 2006), and influence micrometeorology and regional weather patterns (Oke, 1982; Zhang et al., 2004; Zhou et al., 2011).

The process of urban development results in immediate losses of vegetation, however, after initial land conversion, urban land cover gradually becomes composed of heterogeneous patches of impervious surfaces, buildings, street trees, urban forests, and managed green spaces (Goetz et al., 2003; Luck and Wu, 2002; Zhou and Troy, 2008). Although urban areas are the major centers for energy consumption and emissions of CO_2 (IEA, 2008), they also sequester some of the very same emissions they produce; namely in urban soils and foliar and woody biomass (Imhoff et al., 2004; McPherson et al., 2005; Golubiewski, 2006; Raciti et al., 2011; Briber et al., 2013). Urban vegetation can also aid in local carbon mitigation strategies (Nowak and Crane, 2002; McPherson et al., 2005). Though potential urban carbon sinks are likely to be modest, urban vegetation functions as a vital component of urban ecosystems and the carbon cycle while also providing aesthetic, economic, and ecological value to urban dwellers (Nowak and Crane, 2002; Raciti et al., 2012).

Tree cover makes up a significant portion of land cover within the urban mosaic, with proportions in major US cities ranging from ~10 to 54% of land area (Nowak and Greenfield, 2012). However, 'urban' is a unique and inconsistently defined land cover that can store large stocks of carbon. For example, Raciti et al. (2012) compared three commonly used urban definitions and found that vegetation carbon stock density estimates ranged from 37 ± 7 to 66 ± 8 Mg C ha^{-1} for the urban portions of the Boston metropolitan area. Hutyra et al. (2011b) found an average of 89 ± 22 Mg C ha^{-1} (57% mean canopy cover) in vegetation within the Seattle Metropolitan Statistical Area lowlands, a region that is home to over 3.2 million people. This vast range in urban C stock estimates reflects both ambiguous definitions of urban and urban land cover heterogeneity itself.

Societal benefits of urban forest, like urban forest extent itself, are not equally distributed within and across metropolitan areas (Iverson and Cook, 2000; Flocks et al, 2011; Szantoi et al, 2012). Szantoi et al. (2012) found that urban tree cover was related to ethnicity, age, education level, mean annual household income, and housing tenure in Miami-Dade County, Florida. Heynen et al. (2006) found that lower household incomes, a higher proportion of renters, and a higher proportion of minority residents were all correlated with lower residential tree canopy cover in Milwaukee, WI. The ability to accurately map urban tree cover, combined with the use of quantitative tools such as the tree Priority Planting Index (Nowak and Greenfield, 2008), can assist communities in locating areas where urban greening initiatives will have the largest positive influence on communities (Raciti et al., 2006).

Researchers have used satellite data to monitor deforestation, map biomes, and extract vegetation characteristics such as Leaf Area Index (LAI) and plant productivity. Recent studies have begun to extract important functional characteristics such as biomass, phenology, and plant productivity for urban vegetation (Zhang et al., 2004; Myeong et al., 2006; Diem et al., 2006; O'Neil-Dunne et al., 2012). Myeong et al. (2006) used Landsat TM imagery from Syracuse, NY to quantify the aboveground carbon storage of urban trees by using ground samples and a US Forest Service (USFS) urban tree model to estimate per pixel biomass. The agreement between a Normalized Difference Vegetation Index (NDVI) and biomass in Syracuse was significant, but 30 m resolution Landsat data lacks the detail needed for accurate urban vegetation mapping, including the ability to differentiate between lawns, shrubs, and trees, which vary considerably in their contribution to above ground biomass.

Very high resolution imagery from the commercial satellites IKONOS and QuickBird have been used to map urban vegetation in many cities worldwide including Hong Kong (Nichol and Wong, 2007), Vancouver, BC (Tooke et al., 2009), Kuala Lumpur (Chen et al., 2009), and Los Angeles (McPherson et al., 2013). Some of the more recent works have integrated LiDAR data to further refine classification accuracies (Chen et al., 2009; Huang et al., 2013). Segmentation and object-oriented approaches have also been used to identify species in the urban canopy. Walker and Briggs (2007) used 0.6 m true color digital aerial photography and an object oriented analysis to classify urban vegetation and various genera in Phoenix, AZ. Despite the availability of only 3 spectral bands, they were still able to map urban vegetation with an accuracy of 81% and differentiate between species with moderate success. With the exception of the work done by Myeong et al. (2006), Nowak and Crane (2002), Hutyra et al. (2011a), and Davies et al. (2011, 2013), few studies have used remote sensing to estimate biomass in urban environments. None of the aforementioned studies provided biomass maps that are spatially explicit beyond the location of broad land use or vegetation classes, for which a single mean biomass value was applied. LiDAR-based tree height data have been used to estimate biomass in forested systems (e.g. Kellndorfer et al., 2013), but these data have not been widely used to model tree biomass in urban areas beyond the identification of broad vegetation types (e.g. Davies et al., 2011).

Spatially detailed maps of urban vegetation represent an important tool for urban forest management and for the modeling of biogenic carbon dynamics and ecosystem services within urban systems. In this paper, we demonstrate 1) how combining multisource, very high resolution remotely sensed data can help improve the mapping of tree canopy cover, 2) how LiDAR-based tree height metrics can be used to estimate tree biomass in urban areas, 3) how the spatial scale of remote sensing data influences our ability to resolve urban biomass, and 4) how patterns of biomass in the City of Boston differ across neighborhoods with widely varying demographic characteristics.

2. Methods and data

Detailed below is our approach to estimating urban tree biomass using multiple remotely sensed data sources. We developed a multi-level segmentation process to delineate crown and canopy area using a combination of QuickBird imagery and LiDAR point cloud data. Direct field measurements of tree diameters and allometric scaling were used in conjunction with the segmented canopies to build a height-based model of urban tree biomass. Model estimates were validated using both open-grown and closed-canopy trees.

2.1. Site description

Our analysis focused on Boston, Massachusetts (42.356°N, −71.062°W; land area of 125 km^2). Boston is the northernmost city of the largest megalopolis in the United States, which extends from Boston to Washington DC (the 'BosWash corridor'). The 'BosWash' region typifies dispersed urban sprawl style development and is home to 20% of the U.S. population (Schneider and Woodcock, 2008). Like many North American cities, the greater Boston region has experienced significant population growth and subsequent widespread urbanization over the past several decades, most of which has occurred well outside of the urban core. As one of North America's oldest cities, Boston proper has been extensively developed and built-out; however, the City has some of the nation's oldest and most well known parklands and open spaces (e.g. Boston Common and The Emerald Necklace). Boston is commonly classified in the temperate deciduous forest biome and a humid continental climate under the Koppen climate classification system. Native vegetation of the area is dominated by deciduous trees including red oak (*Quercus rubra*), red maple (*Acer rubrum*), sugar maple (*Acer saccharam*), Eastern hemlock (*Tsuga canadensis*), and black cherry (*Prunus serotina*). Similar to many other urban areas, Boston has great diversity in its flora, due to the introduction of exotic,

ornamental and invasive species over the course of centuries (Clemants and Moore, 2003).

2.2. Data sources

Two 4-band, 2.4 m QuickBird images of the greater Boston, MA urban area were acquired from DigitalGlobe Inc., Longmont, CO (Fig. 1A). The image acquisition dates were July 26, 2006 and Aug 3, 2007, during peak growing season, and both images had off nadir angles of 7°, and <1% cloud contamination. Together the two images cover an area of approximately 350 km^2 including all of the City of Boston and parts of Somerville, Cambridge, Chelsea, Everett, Brookline, Newton, Arlington, and Watertown. The Aug 3, 2007 image covers approximately 80% of the study area, with the July 26, 2006 image used to fill in the western portion of the study site. Atmospheric correction and conversion to surface reflectance ($\mu W\ cm^{-2}\ nm^{-1}\ sr^{-1}$) was done with a modified MODTRAN dark object subtraction algorithm, FLAASH (fast line of sight atmospheric analysis of spectral hypercubes; ITT Visual Information Solutions, Boulder, CO). The images were orthorectified using a 1/9 arc sec USGS digital elevation model, projected to UTM zone 19 N, NAD83, and mosaiced with a 500 m mean value stitch overlap.

LiDAR data products, in the form of pre-processed x, y, z point cloud files, were obtained from the Massachusetts Geographic Information System (MassGIS) (Fig. 1B). The data products were delivered as three geospatial layers representing first returns, last returns, and a bare earth model. The data products are based on small footprint (1 m) discrete return data, flown from aircraft during June of 2005 by 3Di Technologies, Inc. Accuracies are reported as 50 cm on the horizontal plane, and 15 cm in the vertical direction. Bare earth, first return and last return point cloud data were interpolated to 1 m rasters for the extent of the QuickBird dataset. A normalized digital surface model (nDSM) was created by subtracting the bare earth model from the first return layer. Fig. 1 shows spatial extent and site details for the LiDAR and QuickBird datasets.

Land use/land cover data was obtained from the 2005 Massachusetts Land Cover data layer, a statewide, seamless digital data set created using semiautomated methods and based on 0.5 m resolution digital orthoimagery from April 2005 and enhanced with assessor parcel and other ancillary data (MassGIS, 2009). Secondary canopy cover estimates were obtained from the 2006 National Land Cover Dataset as a coarser resolution (30 m) point of comparison with the higher resolution canopy estimates that we generated as part of this work (NLCD; Fry et al., 2011). A 1 m resolution Impervious Surface Area (ISA) data layer was obtained from MassGIS (2009). The ISA layer was based on 0.5 m resolution near infrared orthoimagery that was acquired in April 2005 and road network data. Impervious areas included constructed surfaces, such as buildings, roads, asphalt, and manmade compacted soil. Neighborhood-level demographic data on income, race, education, housing tenure, and other parameters were based on 2010 US Census data compiled by the Boston Redevelopment Authority (BRDA) Research Division (Boston Redevelopment Authority, 2013). In all

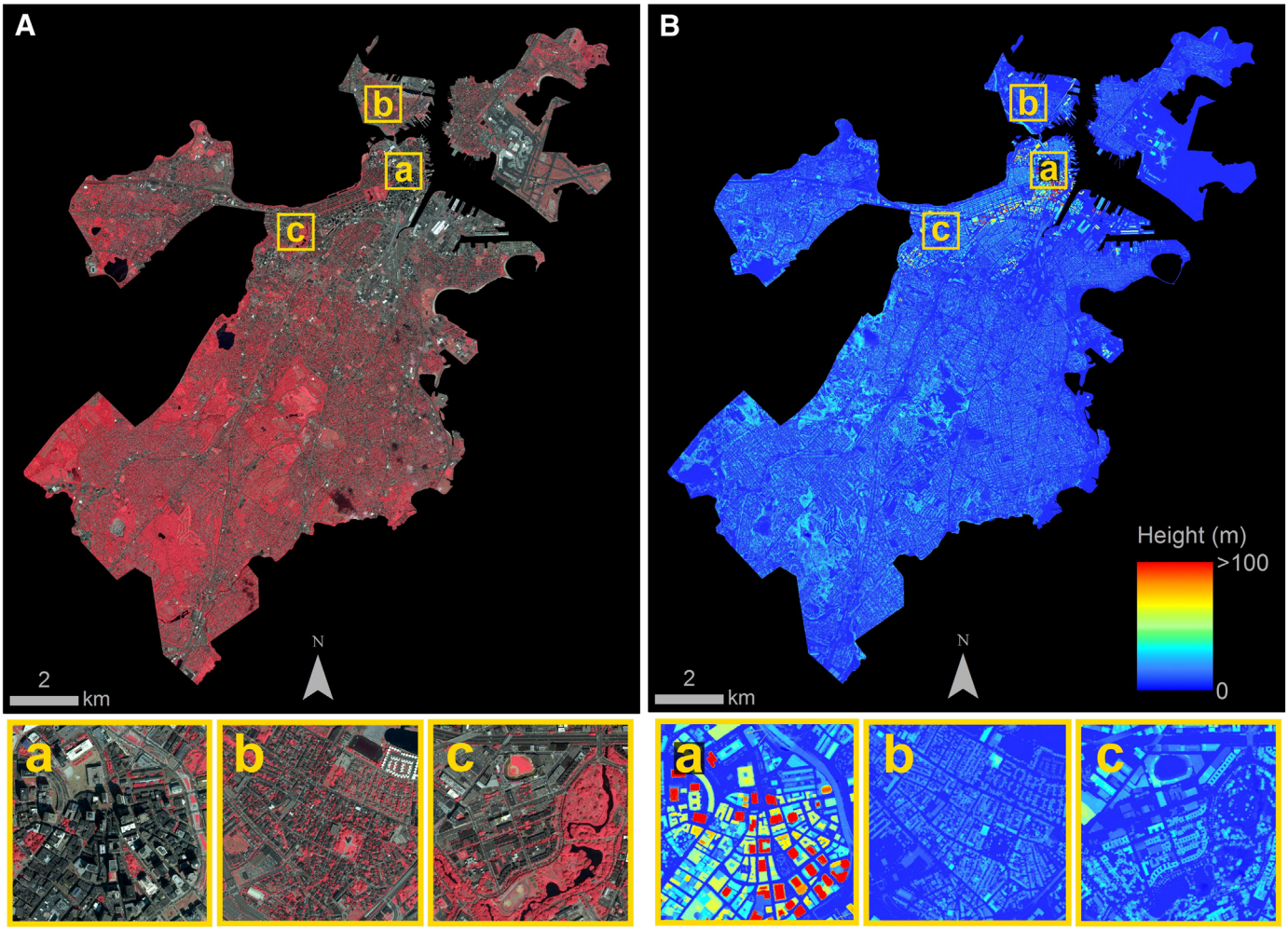

Fig. 1. QuickBird imagery (A, left) and a normalized difference surface model based on LiDAR (B, right) for the City of Boston. The QuickBird imagery is displayed in false color (red = NIR, green = red, blue = green), while the LiDAR first return is shaded from blue (low elevation) to red (high elevation). The close-up examples illustrate the Central (a), Charlestown (b), and Fenway-Kenmore (c) neighborhoods, respectively. (For interpretation of the references to color in this figure legend, the reader is referred to the web version of this article.)

cases, the smallest census geographic unit was used (block, blockgroup, or tract level) to apportion the data to neighborhoods. In cases where a census geographic unit was split between neighborhoods, the 2010 block-level population data were used to apportion the populations. Please see the original BRDA report for further details (Boston Redevelopment Authority, 2013).

2.3. Identification of urban vegetation using multi-source remotely sensed data

To facilitate reproducibility, the classification scheme for mapping Boston's urban canopy was kept computationally simple through a process of rule-based thresholding. The first step involved calculating a normalized difference vegetation index (NDVI), which is a measure of greenness that is strongly correlated with vegetation cover. For QuickBird imagery NDVI was calculated as the difference in surface reflectance between the NIR (Band 4) and red band (Band 3), divided by the sum of the NIR and red bands:

$$NDVI = \frac{\rho(\lambda_{NIR}) - \rho(\lambda_{NIR})}{\rho(\lambda_{NIR}) + \rho(\lambda_{RED})} \quad (1)$$

All pixels with NDVI greater than 0.1 were considered to have significant amounts of vegetation and were included in the analysis; pixels with NDVI <0.1 were excluded from subsequent analysis. The NDVI layer was transformed to a binary mask (vegetation = 1, all else = 0) and combined with the 1 m resolution nDSM to create a map of height for all vegetated areas. Vegetated areas less than 1 m in height (grasses and shrubs) were removed, resulting in a representation of the urban tree canopy.

An accuracy assessment was carried out using a class area weighted, stratified random sample of 372 pixels (246 pixels from the non-tree class and 126 from the tree canopy class) and exported into Google Earth for ground-truthing using high resolution imagery. 'Historical imagery' options within Google Earth proved to be particularly useful as validation tools. The final area of the tree canopy map was adjusted to account for the classification errors, and a 95% confidence interval was calculated for the adjusted tree canopy area (Cochran, 1977; Card, 1982).

2.4. Segmentation of urban tree canopy into individual tree crowns

A region-growing segmentation algorithm was used to delineate individual tree crowns within areas identified as tree canopy. Tree crown segmentation was performed using Definiens Developer 8.0 (www.definiens.com), a fuzzy logic and object-based image processing software. The Definiens segmentation algorithms use a region growing method in which seed pixels are selected from the image, merged with neighboring pixels of similar values, and then consolidated into 'image objects' based on pixel values, texture, shape, and object metrics (Baatz and Schäpe, 1999; Benz et al., 2004).

For crown and canopy extraction we employed a multi-tiered, hierarchical segmentation approach in which the initial vegetation height layer was broken down to increasingly smaller segments based on LiDAR nDSM height metrics (e.g. within object mean height and variance). This workflow was developed and tested using to two contrasting study areas: 1) a high-density residential neighborhood with managed parkland; and 2) a larger lower density region, with mixed land-use and extensive managed and unmanaged forest land.

A 'contrast split segmentation' was used to segment the vegetation height layer into image objects, delineating patches of canopy including individual street trees, clusters of trees, and whole forest patches. Segments ranged from 1 m^2 to several km^2 in size. Next, a large-scale 'Multi-resolution segmentation' was run on the contrast split layer, breaking up the image into segments ranging from 1 m^2 to ~1 ha based on the mean, max, and standard deviation of the nDSM heights. At this point segments represented groups of adjacent pixels with similar height values, frequently equivalent to stands of trees. Segments were then classified into 10 classes based on object area and the mean and maximum nDSM height in the object. A 5 × 5 mean pixel filter of the nDSM was given partial weight in the segmentation helping to smooth the canopy layer, and accentuate crown and canopy shape. Class-specific multi-resolution segmentations were then run on each tree stand class using high 'shape parameter' values ranging from 0.80 to 0.95 to assemble compact image objects. The different tiered segmentations were based on the average tree crown diameter observed in each class, and ranged from scale parameters of 2 to 25. This process successfully captured the shape and area of individual, open grown tree canopies (e.g. typical street and lawn trees), but was not always able to distinguish individual tree canopies within continuous areas of canopy when those trees were similar in height, color, and textural properties.

2.5. Development of a height-based model of urban tree biomass

To build a citywide biomass estimate, diameter-based allometric biomass equations from Jenkins et al. (2003) were applied to the City of Boston's street tree database (Urban Ecology Institute, 2008) and used in combination with the segmented tree crowns and LiDAR metrics. The most specific allometric equation possible was used in all cases; where species or genus level equations were unavailable, we applied the Jenkins et al. (2003) miscellaneous hardwood or softwood equations. Please refer to our previous work for the list of specific allometric equations used and how they were applied (Raciti et al., 2012). One half of live plant biomass was assumed to be carbon. Note that results from McHale et al. (2009) and Timilsina et al. (2014) suggest problems with the application of forest-derived allometries to urban trees; however, urban tree allometries were not available for the regional species assemblage. It is unclear if the use of urban-specific allometric equations would have increased or decreased the estimated carbon stocks in the most urban plots; this is an area that requires additional research.

A sample of 404 accurately segmented tree crowns, selected from a mix of open grown trees and areas of contiguous canopy, were used for model development and validation; 284 were used for model parameterization and 120 were reserved for validation purposes. The tree-level biomass estimations from the street tree database were linked to their respective crown polygon (segment) and then LiDAR nDSM statistics were extracted for each object (tree) including: maximum, minimum, and mean height returns, standard deviation, segment area, and volume (e.g. sum of 1 m resolution height pixels). A range of LiDAR-based metrics was tested using both pixel and object-based regression models (including linear, exponential, logistic, etc.).

Our initial model used the relationship between object volume and biomass to estimate the biomass of individual canopy segments, but this method proved problematic for two reasons: 1) a substantial proportion of segmented tree canopies within areas of contiguous canopy cover were not accurately delineated and 2) a pixel-based model using canopy height was simpler and provided similar predictive power. This simpler pixel-based model based on a linear regression of tree biomass and height for correctly delineated tree canopies, proved robust in a range of urban planting conditions (see Results & discussion). The empirical equation derived from this regression relationship was:

$$B = 2.1015 * H + 0.8455 \quad (2)$$

where B is biomass in kg and H is canopy height in m for a 1 m^2 canopy pixel. The advantage of this simple height-based model was that it could be applied across all canopy areas, even in locations where our segmentation algorithm failed to correctly delineate the boundaries between individual tree canopies. While few studies have used remote sensing

to estimate biomass in urban areas, height-based biomass models have been successfully employed in a number of forest studies (Hyyppa et al., 2001; Popescu et al., 2004; Kellndorfer et al., 2013).

2.6. Field validation of the biomass model

Measurements of tree diameters and allometrically-based biomass estimates were used for model parameterization and validation. Field measurements came from two sources (1) 120 street trees from a city-wide street tree inventory provided by the Massachusetts Office of Geographic Information (MassGIS) and the Boston Parks Department; and (2) 73 randomly located field plots of varying sizes spread across the city. The street tree data were collected in 2005 and 2006 and included information on species, diameter at breast height (DBH), height range, health, and GPS coordinates for each tree. To supplement the street tree dataset with a more varied sample of trees, we collected additional data from 73 field plots. Forty-six of these field plots were randomly selected stands of urban trees ranging from 5 to 534 m^2 in canopy area (median canopy area = 75 m^2). The remaining 27 field plots were 30 m diameter circles (median canopy area = 106 m^2) containing a mix of open-grown trees and small stands surveyed in 2010 as part of a stratified random sampling design that included a range of land uses and development intensities (Raciti et al., 2012). All live trees larger than 5 cm in DBH were surveyed in each field plot. DBH was measured at 1.37 m unless slope or tree form abnormalities required adjustments; measurements followed the protocols outlined in Fahey and Knapp (2007). For the fixed radius plots, trees were identified to species or genus (if species could not be determined). Biomass of live trees was estimated using published allometric equations relating plant diameter to dry mass (please refer to Section 2.5).

2.7. Biomass, demographic characteristics, and the Priority Planting Index

We explored relationships between our estimates of neighborhood level biomass and demographic data from the 2010 US Census (Boston Redevelopment Authority, 2013) using linear regression with appropriate tests for normality and homoscedasticity. All statistics were performed using SAS JMP 9.01 (SAS Institute, Cary, NC). The demographic characteristics evaluated included population density, race, median household income, educational attainment, and housing tenure (the proportion of residents who rent versus own their housing unit).

We also examined regression-based correlations between demographic characteristics and the Priority Planting Index (PPI), which is a tool developed by the USDA FS to determine priority areas for tree planting that will provide the greatest societal benefit (Raciti et al., 2006; Nowak and Greenfield, 2008). The index has three weighted components: population density, existing tree stocking levels, and existing tree cover per capita. The greater the population density, the lower the tree stocking levels, and the lower the existing tree canopy per capita, the higher the PPI score for that neighborhood. Neighborhood-level population density was obtained from 2010 US Census data compiled by the Boston Redevelopment Authority (2013). Existing tree canopy was estimated based on the new data layers derived in this study. A tree stocking level represents the proportion of potentially available planting space currently occupied by tree canopy cover and includes all non-impervious surface areas not presently covered by tree canopy. Note that potential planting areas are not all necessarily *desirable* planting areas and do not take into account the possibility of removing impervious surfaces to plant trees. Tree stocking levels provide a rough metric that allows us to compare potential planting space between neighborhoods. We calculated tree stocking levels based on a high resolution (1 m) impervious surface layer obtained from MassGIS (2009) and the aforementioned urban tree canopy layer. The PPI was calculated for each Boston neighborhood with each of the three index criteria standardized on a 0 to 1 scale, with 1 representing the neighborhood with the highest value in relation to priority of tree planting. Individual scores were combined and standardized based on the following formula to produce an overall PPI value between 0 and 100 such that

$$\mathrm{PPI} = (\mathrm{PD} * 40) + (\mathrm{TS} * 30) + (\mathrm{TPC} * 30). \quad (3)$$

PD is standardized population density, TS is standardized tree stocking levels, and TPC is standardized tree cover per capita. The resulting value for PPI is then standardized again, with the highest value equal to 100 (highest priority for planting).

2.8. Comparison with coarser resolution biomass mapping products

We compared our biomass map for the City of Boston to two coarser-resolution biomass maps that have national coverage, the National Biomass and Carbon Dataset (NBCD 2000) and the United States Department of Agriculture Forest Service (USDA FS) Forest Inventory and Analysis (FIA) biomass map for the contiguous United States (FS-FIA from here forward) (Kellndorfer et al., 2013; Blackard et al., 2008). The goal of these comparisons was to 1) determine how maps based on traditional forest inventories compare to an urban-based product, 2) to examine how the scale of the underlying remote sensing data (1 m, 30 m, and 250 m) influences estimates of urban forest biomass, and 3) to investigate the influence of using a discrete land use or land cover based map to estimate biomass.

Both the NBCD 2000 and FS-FIA biomass maps are based on traditional forest inventory data and were not specifically designed to capture biomass in urban areas, but provide spatially continuous biomass estimates that include the City of Boston. The National Biomass and Carbon Dataset (NBCD 2000) is a 30 m resolution biomass map for the year 2000 that is based on the relationship between canopy height, proportion of canopy cover, and field measured biomass across 66 ecoregions in the contiguous United States (Kellndorfer et al., 2013). The canopy height estimates used in the NBCD 2000 are based on data from the year 2000 Shuttle Radar Topography Mission. The proportion of canopy cover within each pixel is taken directly from the National Land Cover Dataset (NLCD) 2001 Canopy layer. In areas where the NLCD 2001 Canopy layer provides a non-zero canopy estimate, the NBCD 2000 product provides a biomass estimate based on height, canopy cover, and ecoregion. The field data used to define the empirical relationship between canopy height and biomass in each ecoregion are derived from the Forest Inventory and Analysis (FIA) database.

The FS-FIA biomass map for the contiguous United States has a spatial resolution of 250 m and is based on the relationships between forest biomass data collected on FIA sample plots and more than sixty geospatially continuous predictor layers (Blackard et al., 2008). These predictor layers include digital elevation models (DEM) and DEM derivatives, Moderate Resolution Spectroradiometer (MODIS) multi-date composites, vegetation indices and continuous vegetation fields, and summarized PRISM climate data.

We extracted biomass data from our very high resolution biomass map, NBCD 2000, and the FS-FIA maps for the City of Boston. We also extracted biomass for 7 condensed land use/land cover classes, which were based on an original 34-class land use/land cover layer developed by the MassGIS (2009). The seven condensed classes were: residential; commercial; industrial; parks, recreation and developed open space; forests and forested wetlands; other natural areas (mainly herbaceous and salt water wetlands); and other developed areas (mainly transportation).

Finally, we compared our very high resolution, remote-sensing-based biomass map to a land-use-based map developed by Raciti et al. (2012). The map from Raciti et al. (2012) was based on field data from 139 plots distributed across 9 land use/land cover classes in the greater Boston region. The mean biomass of each land use/land cover class applied to its respective land area to yield a map of biomass for the City of Boston.

3. Results & discussion

Detailed tree cover maps can provide valuable information to urban foresters, city planners, community groups, and other stakeholders who hope to improve the environment and quality of life in urban areas (McPherson et al., 1997). A number of studies have explored the relationship between tree canopy cover or green space and community composition to better understand how the societal benefits of trees are distributed across urban areas (Iverson and Cook, 2000; Perkins et al., 2004; Landry and Chakraborty, 2009; Boone et al., 2010), but few studies have explicitly addressed the link between tree biomass and the demographic characteristics of urban neighborhoods (e.g. Dobbs et al., 2011). This may be due to the challenges of creating spatially explicit maps of urban forest biomass (Davies et al., 2011, 2013). Most complete censuses of urban trees take place within the public right of way, but these trees typically account for only a fraction of the urban forest (Galvin et al., 2006). Other studies have examined urban biomass on public and private lands in particular cities, but these studies have been based on field plot data that were extrapolated across the entire city based on a single mean biomass value for each land use, land cover or vegetation class (Hutyra et al., 2011b; Davies et al., 2011; Raciti et al., 2012; Nowak et al., 2013). This approach does not provide spatially explicit information about the distribution of biomass beyond the distribution of the land cover classes.

In this work, we demonstrate that 1) using multi-source remotely sensed data can help improve the mapping of both tree canopy cover and biomass, 2) the spatial scale of remote sensing data strongly influences our ability to resolve urban biomass, 3) biomass maps based on discrete land cover classes can provide reasonable estimates at city or neighborhood scales, but may not provide the fine-scale information needed to guide urban greening initiatives, and 4) patterns of biomass in the City of Boston are complex and not readily explained by the demographic characteristics of neighborhoods.

3.1. Accuracy assessment of the urban canopy and tree biomass maps

An accuracy assessment of our canopy cover map yielded a map accuracy of 87.4% and a Kappa coefficient of 0.73, which takes into account 14% variability in class accuracy occurring by chance. This yielded an adjusted tree canopy area of 31.8 $km^2 \pm 1.83$ km^2 or 25.5% ± 1.5% of the total Boston city area. The primary sources of inaccuracy in the canopy layer were errors of commission that were a result of a scale mismatch between object and pixel (i.e. the mixed pixel problem, wherein the size of a single pixel is larger than the objects under study). A large portion of the mixed pixel error was observed along the edges of buildings with adjacent turf or shrub cover. In these cases, the green area of the turf or shrub layer was coincident with the estimated height of the edge of a building's roof, resulting in the misclassification of these pixels as tree canopy. Another observed source of error was due to the difference in collection dates between the LiDAR and QuickBird data (2005 and 2007, respectively). Some trees had been removed during the two-year period, but of particular note was the confounding influence of the 'Boston Big Dig' on LiDAR returns during construction of the main traffic tunnel (circa 2005) and on NDVI following the creation of a new greenway in place of the formerly elevated highway (circa 2007). Errors of this kind could be greatly minimized in the future through better temporal coordination of the remote sensing data.

We tested the accuracy of our tree biomass map using field measurements from 120 individual trees from the City of Boston street tree inventory and 73 field plots and found strong agreement between field-estimated and modeled biomass ($R^2 = 0.72$, $p < 0.001$ and $R^2 = 0.79$, $p < 0.001$, respectively). In both cases, the regression relationships between field-estimated and modeled biomass were linear and close to 1:1 (Fig. 2). These results demonstrate that the model predictions were robust, despite the wide range of site conditions represented in the field data. These site conditions included street trees, open grown lawn trees, small stands of trees with overlapping canopies, and relatively large forest patches in Franklin Park and the Forest Hills neighborhood.

3.2. Comparison with a single-source very high resolution canopy cover map for the City of Boston

The 'Grow Boston Greener Project' was established in 2006. One of its goals was to improve the quality of urban living by increasing Boston's tree cover to 35% by planting 100,000 trees by 2020. According to an Urban Forest Coalition (UFC) report, Boston's mean forest canopy cover in 2006 was 29%. This estimate was derived from a subcontracted independent analysis using a street tree inventory and 1 m color IR aerial imagery (Urban Ecology Institute, 2008). For the purposes of the present study, the UFC's analysis serves as a comparison of methodological approaches.

Our QuickBird-LiDAR approach resulted in an estimated 25.5% ± 1.5% canopy cover for the City of Boston, which is lower than the 29% estimate from the UFC analysis. A comparison of the two tree canopy layers shows significant overestimation of canopy cover in the UFC product. The largest and most obvious source of error in the UFC layer is the misclassification of grass and shrubs as tree canopy, resulting in an overestimation of tree cover in areas with low-lying vegetation. For instance, the UFC product classifies much of the lawn area on the Boston Common and all of the lawn area within the baseball field at Fenway Park as tree canopy, whereas our data fusion approach correctly characterized these areas as non-canopy due to their low height.

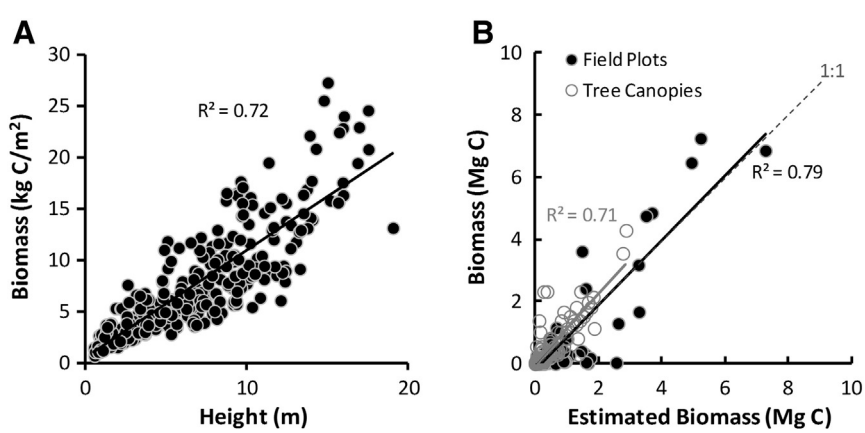

Fig. 2. (A) The relationship between biomass and canopy height for 284 urban trees was used to develop a remote-sensing-based model of urban tree biomass. (B) Agreement between modeled and field estimated biomass. Open circles represent field data from 120 individual trees. Closed circles represent data from 73 field plots from a wide range of growing conditions.

3.3. Distribution of biomass by land use/land cover type

The biomass map developed in this study (Fig. 3) affirms that urban ecosystems can have potentially large aboveground tree carbon stocks, but that these C stocks are heterogeneously distributed across land use/land cover types (Table 1) (Hutyra et al., 2011b; Nowak and Greenfield, 2012; Raciti et al., 2012). We estimated a mean biomass of 28.8 Mg C ha^{-1} and total C storage of 355 Gg C for trees in the City of Boston. For comparison, the City contains approximately one-fourth as much biomass as the nearby Harvard Forest in Petersham, MA (115 Mg C ha^{-1}; Urbanski et al., 2007) and half as much biomass as Northeast and Mid-Atlantic timberlands (mean = 55.4 Mg C ha^{-1}) on a per-unit-area basis (Birdsey et al., 1992). Within the City, urban forest patches contained the largest vegetation carbon stocks on a per-area basis (110.7 Mg C ha^{-1}), followed by residential (32.8 Mg C ha^{-1}), and then parks, recreation, and developed open spaces (23.5 Mg C ha^{-1}). Residential land uses covered 41% of total land area and contained the largest proportion of the total C stocks (46.7%). Urban forest patches covered 8.4% of the land area and contained 32.2% of total C stocks in the City.

3.4. Influence of spatial resolution on estimates of urban forest biomass

We compared estimates from our very high resolution urban biomass map with coarser resolution forest biomass maps, including the NBCD 2000 at 30 m spatial resolution and the FS-FIA biomass map at 250 m spatial resolution (Kellndorfer et al., 2013; Blackard et al., 2008). The coarser resolution biomass maps are based on traditional non-urban forest inventories, but provide biomass estimates within the densely populated City of Boston. These biomass maps are commonly used to model regional ecosystem processes, including within the highly populated northeastern United States, thus an understanding of the way that they represent urban forest biomass is of considerable importance to understanding the outcomes of these ecosystem models (Elliot et al., 2014). We also compared our very high resolution urban biomass map to a 9-class, land-use-based biomass map from Raciti et al. (2012). The land-use-based biomass map is representative of typical approaches to estimating biomass in urban areas, which involve the collection of field data from a set of discrete land use or land cover classes and then applying a mean biomass value to each class. The objectives of these comparisons were to 1) determine how biomass maps

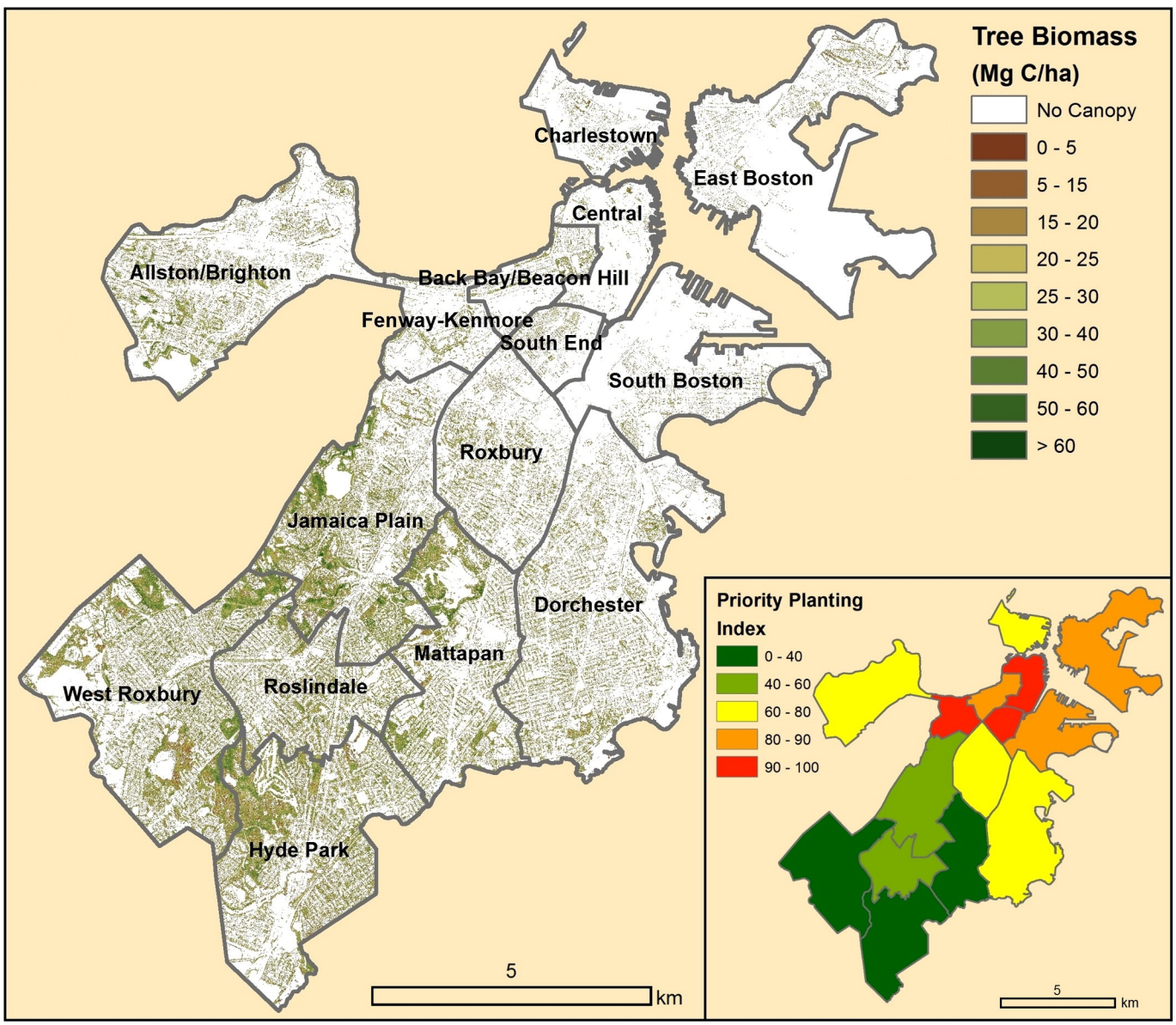

Fig. 3. A very high resolution biomass map for the City of Boston, MA based on the fusion of LiDAR data with QuickBird imagery. Inset: Priority Planting Index (PPI) map by neighborhood.

Table 1
A comparison of tree biomass and canopy cover estimates by land use in Boston, MA. The spatial resolution of the datasets varied from 1 m to 250 m.

Land use	Land area (km^2)	Biomass (Mg C ha^{-1})			Canopy cover (%)	
		1 m (This study)	30 m (NBCD 2000)	250 m (FS-FIA)	1 m (This study)	30 m (NLCD)
Residential	50.6	32.8	14.7	0.3	31.1%	5.7%
Commercial	26.5	13.9	7.6	0.2	14.3%	3.0%
Other developed	15.0	3.5	2.8	0.4	4.4%	1.0%
Parks, recreation & developed open	12.6	23.5	22.9	9.7	22.3%	9.5%
Forest & forested wetlands	10.3	110.7	105.1	15.4	82.5%	59.3%
Industrial	5.3	4.1	1.6	0.0	5.1%	0.4%
Other natural areas	2.4	7.9	25.4	10.2	10.7%	13.5%
City total	123.3	28.8	19.6	2.5	25.5%	9.4%

based on traditional forest inventories differ from an urban-based product, 2) examine how the scale of the underlying remote sensing data (1 m, 30 m, and 250 m) influences estimates of urban biomass, and 3) investigate the affect of using a land-use-based model with discrete classes as the basis for urban biomass mapping.

There are many considerations when choosing an appropriate source of remote sensing data, including the type of environment being studied, available spatial extent, computational requirements for interpreting the data, and four commonly recognized types of sensor resolutions (spatial, spectral, radiometric, and temporal) (Woodcock and Strahler, 1987). These considerations typically involve tradeoffs, for instance, between spatial resolution and the extent of spatial and temporal coverage. Forest biomass mapping has typically been conducted over large spatial extents using sensors with modest resolutions (30 m to 1 km) (Blackard et al., 2008; Ruesch and Gibbs, 2008; Baccini et al., 2008 and 2012; Kellndorfer et al., 2013). Resolving vegetation in urban areas using relatively coarse resolution data presents a range of challenges because urban areas are characterized by fine-scale spatial heterogeneity with major changes in land cover occurring over short distances (Cadenasso et al., 2007). One of these spatial-resolution related challenges is the mixed-pixel problem, wherein the size of a single pixel is larger than the objects under study, leading to the mixing of spectral information from a number of sources (Xiao et al., 2004; Lu and Weng, 2005; Myeong et al., 2006). For instance, a single 30 m pixel pixel that contains an open-grown urban tree is also likely to contain the spectral signatures of nearby lawns, sidewalks, roads, or buildings, thereby confounding the interpretation of the underlying land cover.

Comparing biomass maps, we find strongly decreasing estimates of biomass for the City of Boston as we move from 1 m (28.8 Mg C ha^{-1}, this study) to 30 m (19.6 Mg C ha^{-1}, NBCD 2000) and then to 250 m (2.5 Mg C ha^{-1}, FS-FIA) spatial resolution (Table 1 and Figs. 4 and 5). For forests and parks, which contain areas of continuous canopy, we find strong agreement in the mean biomass estimates for the 1 m resolution and 30 m resolution biomass maps, but the 30 m NBCD 2000 product greatly underestimates biomass for most developed land use classes. The 250 m FS-FIA product severely underestimates biomass in almost all land use/land cover classes within the City of Boston. The exception to this trend is that both the 30 m NBCD 2000 and 250 m FS-FIA products appear to overestimate biomass in non-forested natural areas, possibly due to the misclassification of herbaceous and saltwater wetlands. A recent simulation of this effect by Davies et al. (2013) for Leicester, England shows a similar pattern of decreasing estimates of tree biomass with declining spatial resolution, eventually approaching zero at a pixel size of 1000 m.

A visual comparison of the three maps reveals stark differences in the spatial distribution and density of biomass carbon (Fig. 4). The 30 m resolution NBCD 2000 product reports zero biomass for a large fraction of pixels that clearly contain partial canopy cover when viewed in high resolution imagery. The situation is more severe in the FS-FIA product, which only predicts non-zero biomass for areas with large, continuous expanses of vegetation and tree canopy. In light of the mixed-pixel problem, it is unsurprising that this study and others have demonstrated that relatively coarse resolution ($\geq$30 m) data from sensors such as Landsat, MODIS, and AVHRR tend to underestimate urban tree canopy (Greenfield et al., 2009; Nowak and Greenfield, 2010; Smith et al., 2010; Davies et al., 2013). The comparison is also more complex than it first appears, because while the NBCD 2000 and FS-FIA maps under-estimate biomass at the city-level, they tend to overestimate biomass in the pixels that they classify as containing forest biomass (Fig. 4). The minimum reported biomass in any non-zero pixel was 86 Mg C ha^{-1} for NBCD 2000 and 76 Mg C ha^{-1} for the FS-FIA map, suggesting that all non-zero pixels are being treated as full forests in terms of biomass. We would like to emphasize that the NBCD 2000 and FS-FIA maps provide reasonable, well-validated biomass estimates for rural forested areas over large scales.

This comparison of biomass products appears to imply that higher resolution is better, but working with very high resolution data presents its own set of challenges. The additional spatial detail provided by high resolution imagery permits the mapping of individual objects (for instance individual tree canopies), but also poses the problem of within-class spectral variability caused by shading, shadows, and within object heterogeneity. For example, the sunlit and shaded sides of a tree have very different spectral responses, but belong to the same class and even the same object. This intra-class spectral variability reduces statistical separability between classes when using a traditional pixel based classifier (e.g. maximum likelihood or knowledge-based systems), and creates a salt and pepper effect in the resulting maps, reducing classification accuracy (Jensen, 2000; Chen et al., 2009). A variety of methods have been adopted to deal with within-class spectral heterogeneity, including object-based fuzzy classification (Benz et al., 2004; Herold et al., 2003), and the incorporation of ancillary data, including LiDAR and Geographic Information Systems (GIS) (Hodgson et al., 2003; Câmara et al., 1996). Although there is no single 'best' approach, image segmentation and object-based classification have proven to be among the more robust methods and performed well in this study. Two additional challenges to working with very high resolution data are that data processing can be computationally intensive and the available spatial coverage is likely to be smaller in extent and lower in temporal frequency. For these reasons, coarser resolution remote sensing data will continue to have an important place. A data fusion approach that integrates coarser resolution data for rural areas and higher resolution data for urban areas might provide a good compromise between wide spatial coverage and the ability to resolve the considerable biomass that exists in urban areas.

3.5. Comparison to a biomass map based on discrete land use/land cover classes

We compared our very high resolution biomass map to a nine-class land-use-based map from Raciti et al. (2012) and found very strong agreement at the city (28.8 Mg C ha^{-1} versus 27.9 Mg C ha^{-1}, respectively, Fig. 5A) and neighborhood levels ($R^2 = 0.95$, Fig. 5B). The relationship between the 1 m resolution and land-use-based maps was

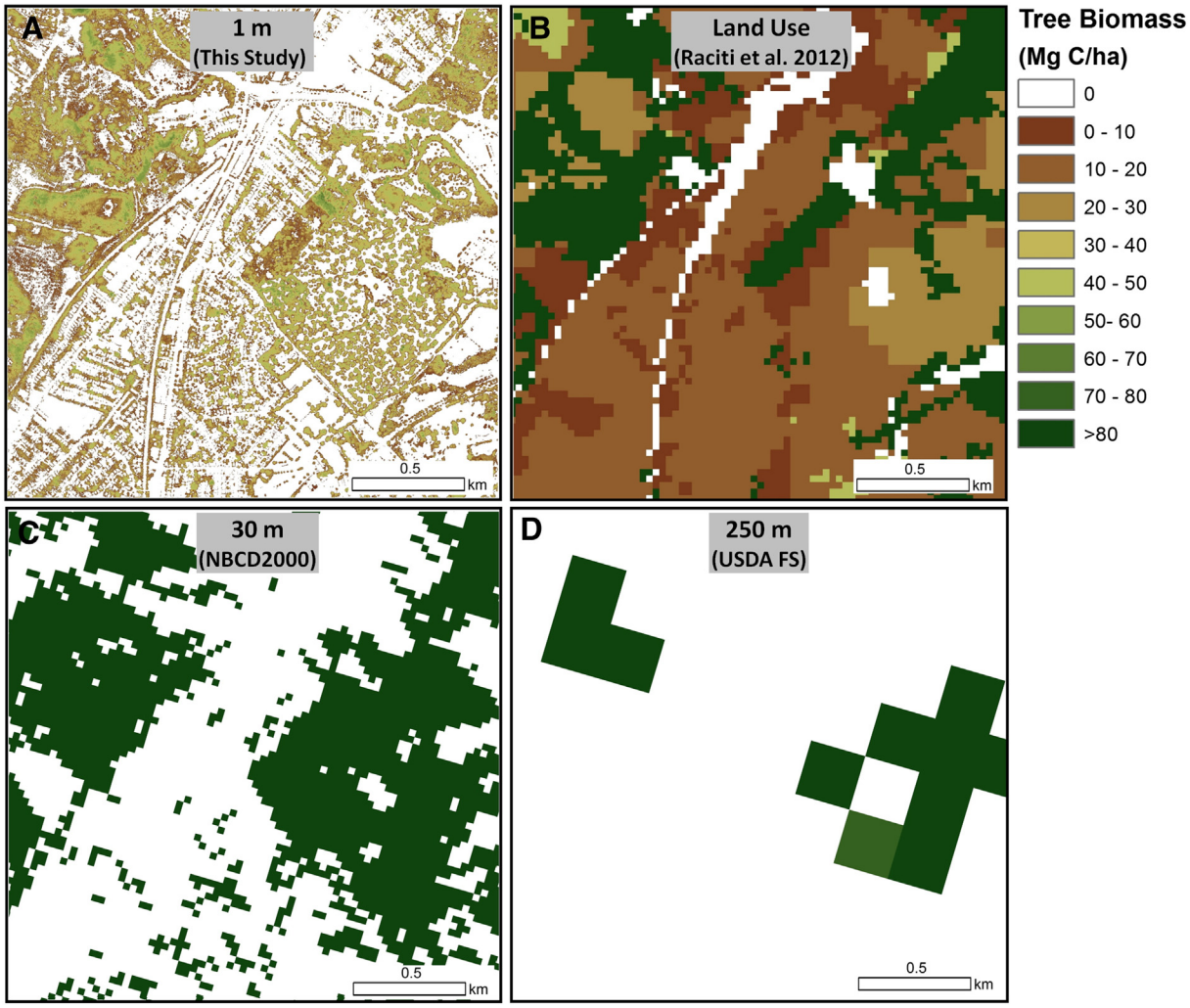

Fig. 4. Comparison of biomass estimates for this study (A), a land use/land cover based estimate (B; Raciti et al., 2012), the NBCD 2000 (C; Kellndorfer et al., 2013), and the USDA FS (D; Blackard et al., 2008).

linear and close to 1:1 at the neighborhood-level (Fig. 5B). This finding suggests that traditional, class-based maps can provide similar biomass estimates to high resolution maps when aggregated at larger spatial scales (e.g. cities or neighborhoods) and when within-class variability is relatively unbiased across the regions of interest. Unfortunately, this approach does not provide the fine-scale information required to inform targeted urban greening initiatives, because a class-based biomass map does not provide spatially explicit information beyond the distribution of the broad land cover/land use types. A map of this type might suggest land use/land cover classes that tend to have lower densities of biomass (e.g. commercial and industrial), but not which particular commercial and industrial areas to target for tree planting.

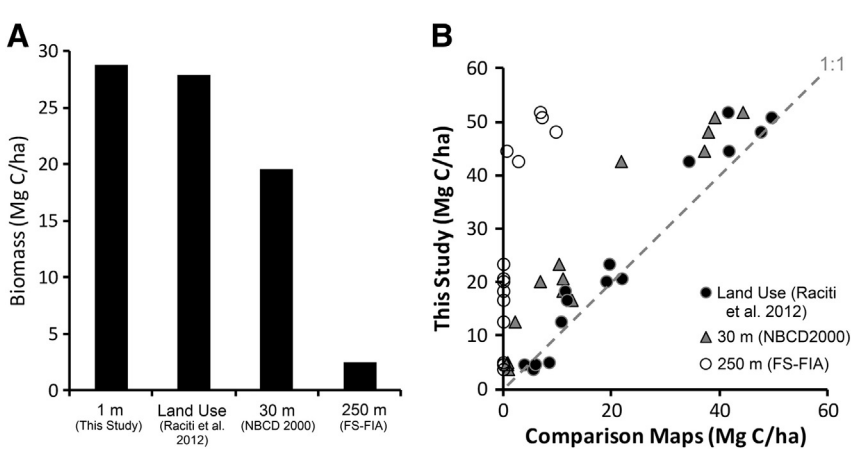

Fig. 5. Comparison of four biomass estimates at the city (A) and neighborhood (B) levels for Boston, MA.

3.6. Biomass by neighborhood demographic characteristics

Urban trees can provide a wide range of ecosystem services, including improved air and water quality, increased property values, lower building energy costs, reduced summertime high temperatures, buffering of wind and noise, and esthetic benefits (McPherson et al., 1997). These societal benefits, like the extent of the urban forest itself, are not equally distributed within metropolitan areas (Iverson and Cook, 2000). There is evidence from a number of cities that neighborhoods with lower incomes and greater proportions of minority residents tend to have disproportionately lower access to trees, parks, and other environmental amenities (Iverson and Cook, 2000; Perkins et al., 2004). For instance, a study in Miami-Dade County, Florida found that predominantly African American and Hispanic areas had lower tree densities than predominantly white areas (Flocks et al., 2011). Similar associations between race or wealth and tree cover have been observed for other cities in the United States (Flocks et al, 2011; Szantoi et al, 2012; Heynen et al., 2006) and internationally (Conway et al., 2011; Escobedo et al., 2006; Kirkpatrick et al., 2007).

One of the surprising results of this study is that, with just one exception (the proportion of renters), we did not find significant (alpha = 0.05) correlations between tree biomass and the demographic characteristics of Boston neighborhoods, including income, education, race, or population density (Supplementary Fig. S1). Some neighborhoods with very high population densities contained high carbon stocks (>50 Mg C ha^{-1}), while others contained relatively little vegetation carbon (<5 Mg C ha^{-1}). In the City of Boston, many of the wealthiest neighborhoods with the highest average educational attainment and lowest proportions of minority residents, contained relatively little tree biomass (Table 2). Conversely, many of the poorest neighborhoods with the highest proportions of minority residents contained very large biomass stocks.

In Boston's neighborhoods, the proportion of households that rent was negatively correlated with urban tree biomass ($R^2 = 0.26$, $p = 0.04$). It is possible that differences in land management or support for urban forest stewardship between renter and owner dominated communities contribute to this trend. Studies in other cities have found negative relationships between the proportion of renters and access to parks, urban forestry resources, and existing tree cover. In Toronto, Canada the intensity of urban forestry activities conducted by resident associations were positively correlated with household income and negatively correlated with the proportion of rented dwellings (Conway et al., 2011). Similarly, most of the urban tree planting associated with the Greening Milwaukee program occurred on owner-occupied properties with relatively little participation from renter-occupied properties (Perkins et al., 2004). An alternative hypothesis is that because Boston is an older city and trees are long-lived, today's neighborhoods have inherited the preferred landscapes of past communities (Boone et al., 2010). For instance, Boone et al. (2010) found that historic demographic patterns were more predictive of urban canopy cover than present-day demographics in Baltimore, MD. Regardless of the reason, it is clear that care must be taken to ensure that the benefits of future urban greening initiatives are equitably distributed (Perkins et al., 2004).

High resolution maps of urban vegetation, combined with quantitative tools such as the tree PPI (Nowak and Greenfield, 2008), can assist communities in locating areas where urban greening initiatives will have the largest positive influence (Raciti et al., 2006). We created a PPI map (Fig. 3, inset) and found that the proportion of renters was correlated with PPI values for Boston neighborhoods ($R^2 = 0.55$, $p = 0.001$). This indicates that neighborhoods with high proportions of renters were also likely to contain high population densities, low tree stocking levels, and low tree cover per capita (the three components of the index score). All of the neighborhoods with the highest index values (80–100) had low tree canopy cover, but clustered into two groups with respect to the other components of the index. One group contained neighborhoods with very high population densities, but relatively high tree stocking levels, indicating limited unpaved land area that can support new trees. It may be challenging to greatly increase tree cover in these areas without also removing impervious surfaces. These neighborhoods included Back Bay-Beacon Hill, Fenway-Kenmore, the South End, and Central (comprised of the smaller China town, Downtown, West End, and North End sub-neighborhoods). The second group of neighborhoods had high PPI scores, in spite of having relatively low population densities, because they had low tree stocking levels. These neighborhoods, which include East Boston and South Boston, have a greater potential for new tree canopy cover. While the PPI is a useful tool, one must use caution in interpreting the results because not all potential planting locations are necessarily desirable planting locations. In the case of East Boston, a considerable proportion of the potential tree planting area surrounds the runways at Boston Logan International Airport.

4. Conclusions

In this paper we integrated remote sensing data and field-based observations to map the canopy cover and estimate the aboveground carbon storage of trees within urban areas at a very high resolution (1 m). We estimated tree canopy cover to be 25.5% ± 1.5% (95% C.I.) and carbon storage to be 355 Gg (28.8 Mg C ha^{-1}) for the City of Boston, demonstrating that even relatively dense urban areas may contain

Table 2
Biomass and demographic characteristics by neighborhood in Boston, MA.

Neighborhoods	Land area (km^2)	This study Biomass (Mg C ha^{-1})	This study Canopy	Population density (km^2)	Median household income	Renters	White alone (race)	Bachelor's degree (25–64 yr old)
Allston/Brighton	11.5	23.4	21.5%	6570	$46,542	79.0%	71.3%	62.7%
Back Bay-Beacon Hill	2.4	18.4	17.8%	11,165	$88,667	66.2%	84.9%	89.3%
Central	3.4	4.7	5.4%	12,281	$70,218	73.0%	72.2%	73.4%
Charlestown	3.5	5.1	6.6%	4660	$89,107	53.7%	80.1%	64.6%
Dorchester	16.2	20.7	20.6%	7046	$44,136	64.5%	26.5%	24.1%
East Boston	12.2	3.8	5.2%	3318	$45,849	72.5%	64.8%	17.8%
Fenway-Kenmore	3.0	16.7	16.1%	13,875	$28,312	91.4%	70.0%	77.7%
Hyde Park	11.9	48.2	44.0%	2585	$58,176	42.4%	34.8%	28.4%
Jamaica Plain	11.6	51.8	42.4%	6055	$54,898	65.1%	60.3%	64.3%
Mattapan	9.2	44.6	36.6%	2457	$41,519	64.5%	8.6%	15.2%
Roslindale	6.5	42.7	38.8%	4420	$61,519	49.5%	56.9%	46.1%
Roxbury	7.4	20.2	20.2%	6533	$31,261	76.8%	18.5%	22.9%
South Boston	8.4	4.7	5.5%	5446	$68,221	59.9%	81.1%	56.9%
South End	1.9	12.7	13.8%	12,875	$46,510	67.0%	60.9%	57.2%
West Roxbury	14.2	50.9	43.1%	2140	$74,797	36.4%	77.2%	55.9%
City of Boston	123.3	28.8	25.5%	5008	$52,065	66.1%	53.9%	46.5%

considerable tree canopy cover and biomass stocks. At present, these urban forest resources are not adequately accounted for in national scale maps of canopy and biomass, which are designed to measure and monitor traditional rural forest resources.

By using high resolution remote sensing data, we were able to provide spatially explicit city-wide estimates of tree biomass and canopy cover. Estimates of this type can fill the gap between the coarse-resolution forest biomass estimates used in rural areas and the limited field-plot-based inventories that are commonly used in cities. The use of multiple sources of remote sensing data allowed us to more accurately distinguish urban trees from low lying vegetation than a previous City-wide analysis that used high resolution imagery alone. The LiDAR data also contained useful information about the structure of urban vegetation, which allowed us to move beyond estimates of urban tree canopy and towards a spatially explicit estimate of urban tree biomass. While previous studies have used very high resolution remote sensing data to provide estimates of urban forest biomass, this is the first study that we know of that provides very high resolution urban biomass estimates that are truly spatially explicit, beyond the application of average biomass values to broad land use/land cover or vegetation types. While we did find strong agreement between the 1 m resolution biomass estimates and the land-use-based estimates at the neighborhood and city scales, the class-based biomass map does not provide spatially explicit biomass information beyond the distribution of the land use/land cover types.

In contrast to studies from other cities, we did not find strong correlations between neighborhood demographics and biomass. Boston is an old and dense city with some of the wealthiest neighborhoods located in areas with the lowest biomass. Our analysis only explored current demographics, but as Boone et al. (2010) found, it is possible that historic demographic characteristics would provide greater explanatory power.

There is growing recognition that urban ecosystems are a vital component in the global carbon cycle and there is a clear need to improve methodological capacity to accurately estimate their carbon budgets (e.g. McPherson et al., 2013). Quantifying the biomass of urban vegetation is an inherently difficult task, given the spatially complex and structurally diverse nature of the urban canopy, and the fundamental limitations of the allometric approach to biomass estimation. Nonetheless, results from this analysis demonstrate that fine-scale estimates can be scaled up to predict biomass across a variety of scales (from individual trees to small stands to entire cities). The techniques described in this paper could be applied in other urban areas and potentially be used for change detection of both biomass and canopy cover. From a research perspective, urban biomass maps can advance our understanding of urban ecological systems and be used as model inputs to analyze landscape function, surface–atmosphere exchanges, and patterns of adjacency between urban and wild forest stands. Detailed urban ecosystem mapping can also be useful for a variety of stakeholders, including city planners, urban foresters, and those wishing to implement green space initiatives and inform policy decisions. Additionally, mapping urban vegetation can provide regional planners with important information to mitigate air pollution, urban heat island effects, and building energy consumption (McPherson et al., 1997). Monitoring and quantifying urban vegetative stocks and carbon fluxes have economic, environmental, and social significance, addressing issues of air quality, climate change, and sustainability.

Supplementary data to this article can be found online at http://dx.doi.org/10.1016/j.scitotenv.2014.08.070.

Acknowledgments

The authors are grateful for the feedback and encouragement provided by Nathan Phillips, Curtis Woodcock, Mark Friedl, and Suchi Gopal. Further, Preeti Rao, Brittain Briber, and Cleo Woodcock provided valuable assistance with field validation. Data for this analysis was provided by the Urban Forest Coalition, DigitalGlobe Inc., and the Massachusetts Geographic Information System. This work was supported by the National Science Foundation for the Boston ULTRA-Ex project to study urban carbon metabolism (DEB-0948857) and an NSF CAREER award (DEB-1149471).

References

Alberti M, Marzluff JM, Shulenberger E, Bradley G, Ryan C, Zumbrunnen C. Integrating humans into ecology: opportunities and challenges for studying urban ecosystems. Bioscience 2003;52:1169–79.

Angel S, Sheppard S, Civco D, Buckley R, Chabaeva A, Gitlin L, et al. The dynamics of global urban expansion, transport and urban development department. Washington, DC: The World Bank; 2005.

Baatz M, Schäpe A. Multiresolution segmentation—an optimization approach for high quality multi-scale image segmentation. In: Strobl J, Blaschke T, Griesebner G, editors. Angewandte Geographische Informations-Verarbeitung XII. Karlsruh: Wichmann Verlag; 1999. p. 12–23.

Baccini A, Laporte N, Goetz SJ, Sun M, Dong H. A first map of tropical Africa's above-ground biomass derived from satellite imagery. Environ Res Lett 2008;3(4):045011.

Baccini A, Goetz SJ, Walker WS, Laporte NT, Sun M, Sulla-Menashe D, et al. Estimated carbon dioxide emissions from tropical deforestation improved by carbon-density maps. Nat Clim Change 2012;2(3):182–5.

Benz UC, Hoffmann P, Willhauck G, Lingenfelder I, Heynen M. Multi-resolution, object-oriented fuzzy analysis of remote sensing data for GIS-ready information. ISPRS J Photogramm Remote Sens 2004;58:239–58.

Birdsey RA. Carbon storage and accumulation in United States forest ecosystems. General Technical Report WO-59. Washington, D.C., USA: USDA Forest Service; 1992.

Blackard JA, Finco MV, Helmer EH, Holden GR, Hoppus ML, Jacobs DM, et al. Mapping US forest biomass using nationwide forest inventory data and moderate resolution information. Remote Sens Environ 2008;112:1658–77.

Boone CG, Cadenasso ML, Grove MJ, Schwarz K, Buckley G. Landscape, vegetation characteristics, and group identity in an urban and suburban watershed: why the 60s matter. Urban Ecosyst 2010;13:225–71.

Boston Redevelopment Authority. Boston in context: planning districts. City of Boston: Boston Redevelopment Authority, Research Division; 2013 [August 15, 2013, http://www.bostonredevelopmentauthority.org/research-maps/research-publications/].

Briber BM, Hutyra LR, Dunn AL, Raciti SM, Munger JW. Variations in atmospheric CO_2 and carbon fluxes across a Boston, MA urban gradient. Land 2013;2(3):304–27.

Cadenasso ML, Pickett TA, Schwarz K. Spatial heterogeneity in urban ecosystems: reconceptualizing land cover and a framework for classification. Front Ecol Environ 2007;5:80–8.

Câmara G, Souza RCM, Freitas UM, Garrido J. Spring: integrating remote sensing and GIS by object-oriented data modeling. Comput Graph 1996;20(3):395–403.

Card DH. Using map category marginal frequencies to improve estimates of thematic map accuracy. Photogramm Eng Remote Sens 1982;49:431–9.

Chen Y, Su W, Li J, Sun Z. Hierarchical object oriented classification using very high resolution imagery and LIDAR data over urban areas. Adv Space Res 2009;43:1101–10.

Clemants SE, Moore G. Patterns of species diversity in eight northeastern United States cities. Urban Habitats 2003;1(1):4–16.

Cochran WG. Sampling techniques. New York, NY: Wiley; 1977.

Conway TM, Shakeel T, Atallah J. Community groups and urban forestry activity: drivers of uneven canopy cover? Landsc Urban Plan 2011;101(4):321–9.

Davies ZG, Edmondson JL, Heinemeyer A, Leake JR, Gaston KJ. Mapping an urban ecosystem service: quantifying above-ground carbon storage at a city-wide scale. J Appl Ecol 2011;48:1125–34.

Davies ZG, Dallimer M, Edmondson JL, Leake JR, Gaston KJ. Identifying potential sources of variability between vegetation carbon storage estimates for urban areas. Environ Pollut 2013;183:133–42.

DeFries RS, Rudel T, Uriarte M, Hansen M. Deforestation driven by urban population growth and agricultural trade in the twenty-first century. Nat Geosci 2010;3:178–81.

Diem JE, Ricketts CE, Dean JR. Impacts of urbanization on land-atmosphere carbon exchange within a metropolitan area in the USA. Climate Res 2006;30:201–13.

Dobbs C, Escobedo FJ, Zipperer WC. A framework for developing urban forest ecosystem services and goods indicators. Landsc Urban Plan 2011;99(3):196–206.

Elliott J, Sharma B, Best N, Glotter M, Dunn JB, Foster I, et al. A spatial modeling framework to evaluate domestic biofuel-induced potential land use changes and emissions. Environ Sci Technol 2014;48(4):2488–96.

Escobedo FJ, Nowak DJ, Wagner JE, Luz De la Maza C, Rodríguez M, Crane DE, et al. The socioeconomics and management of Santiago de Chile's public urban forests. Urban For Urban Green 2006;4:105–14.

Fahey TJ, Knapp AK. Principles and standards for measuring primary production. New York, New York, USA: Oxford University Press; 2007.

Flocks J, Escobedo F, Wade J, Varela S, Wald C. Environmental justice implications of urban tree cover in Miami-Dade County, Florida. Environ Justice 2011;4(2):125–34.

Foley JA, DeFries R, Asner GP, Barford C, Bonan G, Carpenter SR, et al. Global consequences of land use. Science 2005;309:570–4.

Fry J, Xian G, Jin S, Dewitz J, Homer C, Yang L, et al. Completion of the 2006 National Land Cover Database for the Conterminous United States. PE&RS 2011;77(9):858–64.

Galvin MF, Grove MJ, O'Neil-Dunne J. A report on the Baltimore City present and potential urban canopy. Annapolis, MD: Maryland Department of Natural Resources; 2006 [17 pp.].

Goetz SJ, Smith AJ, Jantz C, Wright RK, Prince SD, Mazzacato ME, et al. Monitoring and predicting urban land use change — applications of multi-resolution multi-temporal satellite data. IEEE International Geosciences and Remote Sensing Symposium Proceedings; 2003. p. 1567–9.
Golubiewski NE. Urbanization increases grassland carbon pools: effects of landscaping in Colorado front range. Ecol Appl 2006;16:555–71.
Greenfield ED, Nowak J, Walton JT. Assessment of 2001 NLCD tree and impervious cover estimates. Photogramm Eng Remote Sens 2009;75:1279–86.
Grimm NB, Faeth SH, Golubiewski NE, Redman CL, Wu JG, Bai XM, et al. Global change and the ecology of cities. Science 2008;319:756–60.
Herold M, Liu X, Clarke KC. Spatial metrics and image texture for mapping urban land use. Photogramm Eng Remote Sens 2003;69:991–1001.
Heynen N, Perkins HA, Roy P. The political ecology of uneven urban green space the impact of political economy on race and ethnicity in producing environmental inequality in Milwaukee. Urban Aff Rev 2006;42(1):3–25.
Hodgson ME, Jensen JR, Tullis JA, Riordan KD, Archer CM. Synergistic use of LiDAR and color aerial photography for mapping urban parcel imperviousness. Photogramm Eng Remote Sens 2003;69:973–80.
Huang Y, Yu BL, Zhou JH, Hu CL, Tan WQ, Hu ZM, et al. Toward automatic estimation of urban green volume using airborne LiDAR data and high resolution remote sensing images. Front Earth Sci 2013;7:43–54.
Hutyra LR, Yoon B, Hepinstall-Cymerman J, Alberti A. Carbon consequences of land cover change and expansion of urban lands: a case study in the Seattle metropolitan region. Landsc Urban Plan 2011a;103:83–93.
Hutyra LR, Yoon B, Alberti A. Terrestrial carbon stocks across a gradient of urbanization: a study of the Seattle, WA region. Glob Chang Biol 2011b;17:783–979.
Hyyppa J, Kelle O, Lehikoinen M, Inkinen M. A segmentation-based method to retrieve stem volume estimates from 3-D tree height models produced by laser scanners. IEEE Trans Geosci Remote Sens 2001;39(5):969–75.
IEA. World energy outlook 2008. available from http://www.worldenergyoutlook.org/, 2008.
Imhoff MA, Bounoua L, DeFries R, Lawrence WT, Stutzer D, Tucker CJ, et al. The consequences of urban land transformation on net primary productivity in the United States. Remote Sens Environ 2004;89:434–43.
Iverson LR, Cook EA. Urban forest cover of the Chicago region and it relation to household density and income. Urban Ecosyst 2000;4:105–24.
Jenkins JC, Chojnacky DC, Heath LS, Birdsey R. National-scale biomass estimators for United States tree species. For Sci 2003;49:12–35.
Jensen JR. Remote sensing of the environment: an earth resource perspective. Upper Saddle River, NJ: Prentice-Hall; 2000.
Kaye JP, Groffman PM, Grimm NB, Baker LA, Pouyat RV. A distinct urban biogeochemistry? Trends Ecol Evol 2006;21:192–9.
Kellndorfer J, Walker W, Kirsch K, Fiske G, Bishop J, LaPoint L, et al. NACP aboveground biomass and carbon baseline data, V. 2 (NBCD 2000), U.S.A., 2000. Oak Ridge, Tennessee, U.S.A.: ORNL DAAC; 2013. http://dx.doi.org/10.3334/ORNLDAAC/1161 [Data set, Available on-line [http://daac.ornl.gov] from].
Kirkpatrick JB, Daniels GD, Zagorski T. Explaining variation in front gardens between suburbs of Hobart, Tasmania, Australia. Landsc Urban Plan 2007;79:314–22.
Landry SM, Chakraborty J. Street trees and equity: evaluating the spatial distribution of an urban amenity. Environ Plan 2009;41:2651–70.
Lu D, Weng Q. Urban classification using full spectral information of Landsat ETM + imagery in Marion County, Indiana. Photogramm Eng Remote Sens 2005;71:1275–84.
Luck M, Wu JG. A gradient analysis of urban landscape pattern: a case study from the Phoenix metropolitan region, Arizona, USA. Landsc Ecol 2002;17:327–39.
Massachusetts Office of Geographic Information (MassGIS). Land use and impervious surface datalayers. http://www.mass.gov/anf/research-and-tech/it-serv-and-support/application-serv/office-of-geographic-information-massgis/, 2009. [Last accessed March 26, 2014].
McHale MR, Burke IC, Lefsky MA, Peper PJ, McPherson EG. Urban forest biomass estimates: is it important to use allometric relationships developed specifically for urban trees? Urban Ecosyst 2009;12:95–113.
McPherson GE, Nowak D, Heisler G, Grimmond S, Souch C, Grant R, et al. Quantifying urban forest structure, function, and value: the Chicago Urban Forest Climate Project. Urban Ecosyst 1997;1:49–61.
McPherson G, Simpson JR, Peper PJ, Maco SE, Xiao QF. Municipal forest benefits and costs in five US cities. J For 2005;103:411–6.
McPherson GE, Xiao Q, Aguaron E. A new approach to quantify and map carbon stored, sequestered and emissions avoided by urban forests. Landsc Urban Plan 2013;120:70–84.
Myeong S, Nowak DJ, Duggin MJ. A temporal analysis of urban forest carbon storage using remote sensing. Remote Sens Environ 2006;101:277–82.
Nichol J, Wong MS. Remote sensing of urban vegetation life form by spectral mixture analysis of high resolution IKONOS satellite images. Int J Remote Sens 2007;28:985–1000.
Nowak DJ, Crane DE. Carbon storage and sequestration by urban trees in the USA. Environ Pollut 2002;116:381–9.
Nowak JD, Greenfield EJ. Urban and community forests of New England (General Technical Report NRS-38). Northern Research Station, Syracuse, NY: USDA Forest Service; 2008.
Nowak DJ, Greenfield EJ. Evaluating the National Land Cover Database tree canopy and impervious cover estimates across the conterminous United States: a comparison with photo-interpreted estimates. Environ Manag 2010;46:378–90.
Nowak DJ, Greenfield EJ. Tree and impervious cover change in US cities. Urban For Urban Green 2012;11(1):21–30.
Nowak DJ, Greenfield EJ, Hoehn RE, Lapoint E. Carbon storage and sequestration by trees in urban and community areas of the United States. Environ Pollut 2013;178:229–36.
O'Neil-Dunne JPM, MacFaden SW, Royar AR, Pelletier KC. An object-based system for LiDAR data fusion and feature extraction. Geocarto International; 2012. http://dx.doi.org/10.1080/10106049.2012.689015.
Oke TR. The energetic basis of the urban heat island. Q J Roy Meteorol Soc 1982;108:1–24.
Pataki DE, Alig RJ, Fung AS, Golubiewski NE, Kennedy CA, McPherson EG, et al. Urban ecosystems and the North American carbon cycle. Glob Chang Biol 2006;12:2092–102.
Perkins HA, Heynen N, Wilson J. Inequitable access to urban reforestation: the impact of urban political economy on 'and urban forests. Cities 2004;21:291–9.
Popescu Sorin C, Wynne Randolph H, Scrivani John A. Fusion of small-footprint lidar and multispectral data to estimate plot-level volume and biomass in deciduous and pine forests in Virginia, USA. For Sci 2004;50:551–65.
Potere D, Schneider A. A critical look at representations of urban area in global maps. GeoJournal 2007;69:55–80.
Raciti SM, Galvin MF, Grove JM, O'Neil-Dunne JPM, Todd A, Claggett S. Urban tree canopy goal setting: a guide for communities. Northeastern Area State and Private Forestry, Chesapeake Bay Program Office, Annapolis, MD: USDA Forest Service; 2006.
Raciti SM, Groffman PM, Jenkins JC, Pouyat RV, Fahey TJ, Pickett STA, et al. Accumulation of carbon and nitrogen in residential soils with different land use histories. Ecosystems 2011;14(2):287–97.
Raciti SM, Hutyra LR, Rao P, Finzi AC. Soil and vegetation carbon in urban ecosystems: the importance of importance of urban definition and scale. Ecol Appl 2012;22(3):1015–35.
Ruesch A, Gibbs HK. New IPCC tier-1 global biomass carbon map for the year 2000. Oak Ridge, Tennessee: Oak Ridge National Laboratory; 2008 [Available online from the Carbon Dioxide Information Analysis Center [[http://cdiac.ornl.gov]].
Sadik N. Meeting the urban population challenge. City Dev Strateg 1999;1:16–23.
Schneider A, Woodcock CE. Compact, dispersed, fragmented, extensive? A comparison of urban growth in 25 global cities using remotely sensed data, pattern metrics and census information. Urban Stud 2008;45:659–92.
Schneider A, Friedl MA, Potere D. Mapping global urban areas using MODIS 500-m data: new methods and datasets based on 'urban ecoregions'. Remote Sens Environ 2010;114:1733–46.
Seto KC, Fragkias M, Guneralp B, Reilly MK. A meta-analysis of global urban land expansion. PLoS ONE 2011;6(8):e23777.
Seto KC, Burak G, Hutyra LR. Global forecasts of urban expansion to 2030 and direct impacts on biodiversity and carbon pools. Proc Natl Acad Sci U S A 2012;109.[16083016088].
Smith ML, Zhou W, Cadenasso M, Grove M, Band LE. Evaluation of the National Land Cover Database for hydrologic applications in urban and suburban Baltimore, Maryland1. J Am Water Resour Assoc 2010;46(2):429–42.
Szantoi Z, Escobedo F, Wagner J, Rodriguez JM, Smith S. Socioeconomic factors and urban tree cover policies in a subtropical urban forest. GISci Remote Sens 2012;49(3):428–49.
Timilsina N, Staudhammer CL, Escobedo FJ, Lawrence A. Tree biomass, wood waste yield, and carbon storage changes in an urban forest. Landsc Urban Plan 2014;127:18–27.
Tooke TR, Coops NC, Goodwin NR, Voogt JA. Extracting urban vegetation characteristics using spectral mixture analysis and decision tree classifications. Remote Sens Environ 2009;113:398–407.
UNFPA. United Nations: state of the world population; 2007.
Urban Ecology Institute. State of the urban forest report. www.urbaneco.org/State%20of%20the%20Urban%20Forest%20Report.pdf, 2008. [accessed July 19, 2009].
Urbanski S, Barford C, Wofsy S, Kucharik C, Pyle E, Budney J, et al. Factors controlling CO_2 exchange on timescales from hourly to decadal at Harvard Forest. J Geophys Res 2007;112. G02020.
Walker JS, Briggs JM. An object-oriented approach to urban forest mapping in Phoenix. Photogramm Eng Remote Sens 2007;73:577–83.
Woodcock CE, Strahler AH. The factor of scale in remote sensing. Remote Sens Environ 1987;21(3):311–32.
Xiao Q, Ustin SL, McPherson EG. Using AVIRIS data and multiple-masking techniques to map urban forest tree species. Int J Remote Sens 2004;25:5637–54.
Zhang X, Friedl M, Schaaf CB, Strahler AH, Schneider A. The footprint of urban climates on vegetation phenology. Geophys Res Lett 2004;31:L12209.
Zhou W, Troy A. An object-oriented approach for analyzing and characterizing urban landscape at the parcel level. Int J Remote Sens 2008;29:3119–35.
Zhou WQ, Huang GL, Cadenasso ML. Does spatial configuration matter? Understanding the effects of land cover pattern on land surface temperature in urban landscapes. Landsc Urban Plan 2011;102:54–63.